Progress In Electromagnetics Research, PIER 22, 149–179, 1999

A SPHEROIDAL VECTOR WAVE FUNCTION ANALYSIS OF FIELD AND SAR DISTRIBUTIONS IN A DIELECTRIC PROLATE SPHEROIDAL HUMAN HEAD MODEL

X. K. Kang, L. W. Li, M. S. Leong, and P. S. Kooi

Communications & Microwave Division
Department of Electrical Engineering
National University of Singapore
10 Kent Ridge Crescent, Singapore 119260

1. INTRODUCTION

Recently, there has been an increasing public concern about the health effects of human head exposed to electromagnetic energy emitted from mobile handset antennas. An important motivation for researchers is to gain a detailed understanding of the EM field distribution and power absorption distribution inside the human head [1–3]. There exists a variety of techniques which can be used to perform the required analysis, each with its own strength and weakness. In the analysis, the model obtained from medical imaging serves as a realistic model

but requires a lot of computational time as in the methods of finite element [4], finite difference [5–9] and moments [10, 11]. To increase computational speed, the spherical human head model is also often adopted as an idealized representation of real biological human head in the analysis [12–15], but it is less accurate. In view of the fact that the geometry of a human head can be better approximated by a prolate spheroid than a simple sphere and that the computational time can be saved as compared with those using the Finite Difference Time Domain (FDTD) technique and the Finite Element Method (FEM), a dielectric prolate spheroidal model serves as a compromise for the full-wave analysis of EM field distributions.

The EM waves scattered by a single spheroid or two spheroids have been well-investigated and some analytic solutions have been obtained to date [16–19]. There are, however, only few reports on the analysis of EM field distributions inside the human head based on the prolate spheroidal model, basically due to two difficulties in analyzing the EM fields inside and outside the spheroids. One of the difficulties is the very complicated calculation of the spheroidal angular and radial functions [20, 21]. The other is the difficulty in obtaining analytic solutions of the scattering and transmission coefficients of the TE and TM modes of the EM fields due to the lack of the orthogonality of spheroidal vector wave functions [22, 23]. The perturbation theory has been applied to prolate spheroidal models to obtain internal EM absorbed power distributions, but the convergence is generally slow and the equations are valid only when the semi-axial lengths of the spheroid are much longer than the wavelength [24]. Iskander and Lakhtakia *et al.* have studied the exposure of a prolate spheroidal model to the near field of a short dipole or a small loop antenna, using the spherical vector harmonics and the extended boundary condition method (EBCM) [25–27]. The formulas used in the EBCM failed to provide convergent and accurate results for sources located at very small distances to the model. The recent investigation of the radiated fields inside a prolate spheroidal human body model due to a loop antenna is limited to the scalar analysis and the $\hat{\phi}$-component of fields only [28].

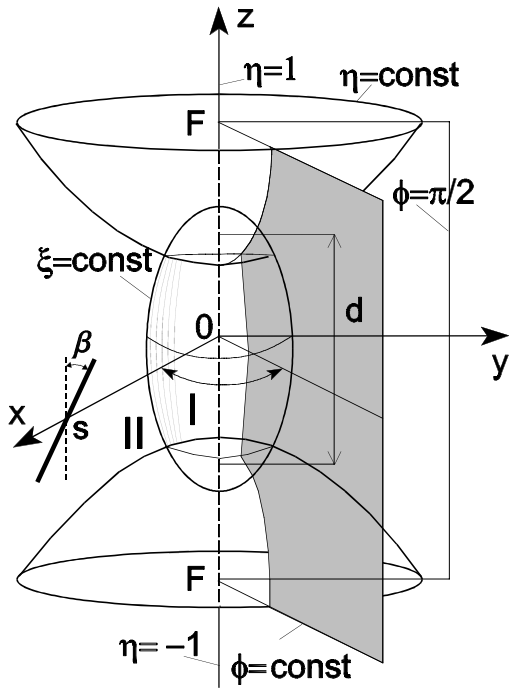

Figure 1. Modeling of the problem.

2. FORMULATION OF THE PROBLEM

2.1 Dielectric Prolate Spheroidal Human Head Model

In the present analysis, the human head together with the mobile handset is modeled as a dielectric prolate spheroid with a dipole antenna positioned a short distance away from it, as shown in Fig. 1, where η is an angular coordinate, ξ is a radial one, and ϕ is an azimuthal one. The focal distance is denoted by d. The regions inside and outside the human head are labeled as I and II, in which the wave propagation constants are k_1 and k_2, respectively. To make reasonable assumptions, the major and minor semi-axial lengths of the spheroid are chosen as 10 cm and 7.5 cm, respectively. The antenna is modeled as a $\lambda/4$ dipole located at a distance of s away from the spheroid. In this paper, two frequencies are studied, namely the GSM

(Pan European Cellular System-Group Special Mobile, the center frequency is 900 MHz) and the PCN (Personal Communications Network, the center frequency is 1800 MHz) frequencies. The dielectric constants of the spheroidal head are chosen as the average values of the tissue parameters at the respective frequencies ($\sigma = 1.25$ S/m and $\epsilon_r = 59$ for GSM; and $\sigma = 1.38$ S/m and $\epsilon_r = 55$ for PCN) [12, 29–31]. For various sources and the boundary surfaces, different confocal spheroids are assumed according to Flammer's formulations for the Green's function in the spheroidal system [20]. To simplify the computation with reasonable assumptions, the orientation of the dipole is chosen to be on the plane paralleled to the zoy plane, and the feed center of the dipole is located at $\eta' = 0$ and $\phi' = 0$. The inclination angle of the dipole is denoted by β, which is the angle between the linear dipole and the z-axis.

2.2 Expansions of EM Fields using Spheroidal Vector Wave Functions

The electromagnetic waves excited by the dipole can be expressed in terms of the appropriate spheroidal vector wave functions by means of the formulated dyadic Green's functions in the spheroidal coordinate system and the method of scattering superposition [32–35] as follows:

$$\begin{aligned}
\boldsymbol{E}_I(\boldsymbol{r}) = \frac{-\omega\mu_1}{2\pi} \sum_{n=m}^{\infty} \sum_{m=0}^{\infty} \Bigg\{ & \left[A_{\substack{o\\e}mn}^{zM} \boldsymbol{M}_{\substack{e\\o}mn}^{z(1)}(c_1,\xi) + A_{\substack{e\\o}mn}^{zM} \boldsymbol{N}_{\substack{o\\e}mn}^{z(1)}(c_1,\xi) \right] \\
& \cdot \iiint_{V'} \frac{2-\delta_{m0}}{N_{mn}} \psi_{\substack{e\\o}mn}^{(3)}(k_2,\xi') I_z(\xi') dV' \\
& + \Bigg[A_{\substack{e\\o}mn}^{+yM} \boldsymbol{M}_{\substack{e\\o}m+1,n}^{+(1)}(c_1,\xi) + A_{\substack{o\\e}mn}^{+yN} \boldsymbol{N}_{\substack{o\\e}m+1,n}^{+(1)}(c_1,\xi) \\
& + A_{\substack{e\\o}mn}^{-yM} \boldsymbol{M}_{\substack{e\\o}m-1,n}^{-(1)}(c_1,\xi) + A_{\substack{o\\e}mn}^{-yN} \boldsymbol{N}_{\substack{o\\e}m-1,n}^{-(1)}(c_1,\xi) \Bigg] \\
& \cdot \iiint_{V'} \frac{2-\delta_{m0}}{N_{mn}} \psi_{\substack{e\\o}mn}^{(3)}(k_2,\xi') I_y(\xi') dV' \Bigg\}, \qquad \text{(1a)}
\end{aligned}$$

$$\begin{aligned}
\boldsymbol{E}_{II}(\boldsymbol{r}) = \frac{-\omega\mu_2}{2\pi} \sum_{n=m}^{\infty} \sum_{m=0}^{\infty} \Bigg\{ & \left[B_{\substack{o\\e}mn}^{zM} \boldsymbol{M}_{\substack{e\\o}mn}^{z(3)}(c_2,\xi) + B_{\substack{e\\o}mn}^{zN} \boldsymbol{N}_{\substack{o\\e}mn}^{z(3)}(c_2,\xi) \right. \\
& \left. + \boldsymbol{N}_{\substack{e\\o}mn}^{z(1)}(c_2,\xi) \right] \cdot \iiint_{V'} \frac{2-\delta_{m0}}{N_{mn}} \psi_{\substack{e\\o}mn}^{(3)}(k_2,\xi') I_z(\xi') dV'
\end{aligned}$$

$$+\left[B_{\substack{e\\o}mn}^{+yM}\boldsymbol{M}_{\substack{e\\o}m+1,n}^{+(3)}(c_2,\xi)+B_{\substack{o\\e}mn}^{+yN}\boldsymbol{N}_{\substack{o\\e}m+1,n}^{+(3)}(c_2,\xi)\pm\boldsymbol{N}_{\substack{o\\e}m+1,n}^{+(1)}(c_2,\xi)\right.$$

$$\left.+\,B_{\substack{e\\o}mn}^{-yM}\boldsymbol{M}_{\substack{e\\o}m-1,n}^{-(3)}(c_2,\xi)+B_{\substack{o\\e}mn}^{-yN}\boldsymbol{N}_{\substack{o\\e}m-1,n}^{-(3)}(c_2,\xi)\mp\boldsymbol{N}_{\substack{o\\e}m-1,n}^{-(1)}(c_2,\xi)\right]$$

$$\cdot\iiint_{V'}\frac{2-\delta_{m0}}{N_{mn}}\psi_{\substack{e\\o}mn}^{(3)}(k_2,\xi')I_y(\xi')dV'\Bigg\}, \tag{1b}$$

where an $\exp(-j\omega t)$ time dependence is assumed for the EM field quantities and it is suppressed throughout the analysis. $A_{\substack{e\\o}mn}^{(z,\pm)M}$, $A_{\substack{e\\o}mn}^{(z,\pm)N}$, $B_{\substack{e\\o}mn}^{(z,\pm)M}$ and $B_{\substack{e\\o}mn}^{(z,\pm)N}$ are unknown coefficients to be determined from the boundary conditions. $I_a=\boldsymbol{I}(\xi')\cdot\hat{\boldsymbol{a}}$ (where $\hat{\boldsymbol{a}}=\hat{\boldsymbol{z}},\hat{\boldsymbol{y}}$), and $\boldsymbol{I}(\xi')$ is the current distribution along the dipole. $\boldsymbol{N}_{mn}$ is the normalization factor of the angular function, and $c_i=\frac{1}{2}k_id\,(i=1,2)$. δ_{mo} is the Dirac delta function. The scalar wave function, $\psi_{\substack{e\\o}mn}^{(i)}$, and the vector wave functions, $\boldsymbol{M}_{\substack{e\\o}mn}^{z(i),\pm(i)}$ and $\boldsymbol{N}_{\substack{e\\o}mn}^{z(i),\pm(i)}$, are defined by Flammer [20]:

$$\psi_{\substack{e\\o}mn}^{(i)}(c,\xi)=\mathcal{S}_n^m(c,\eta)R_{mn}^{(i)}(c,\xi)\begin{matrix}\cos\\\sin\end{matrix}(m\phi), \tag{2}$$

$$\boldsymbol{M}_{\substack{e\\o}mn}^{a(i)}(c,\xi)=\boldsymbol{\nabla}\times\left[\psi_{\substack{e\\o}mn}^{(i)}\hat{\boldsymbol{a}}\right],\qquad\hat{\boldsymbol{a}}=\hat{\boldsymbol{x}},\hat{\boldsymbol{y}},\hat{\boldsymbol{z}}, \tag{3a}$$

$$\boldsymbol{N}_{\substack{e\\o}mn}^{a(i)}(c,\xi)=\frac{1}{k}\boldsymbol{\nabla}\times\boldsymbol{\nabla}\times\left[\psi_{\substack{e\\o}mn}^{(i)}\hat{\boldsymbol{a}}\right], \tag{3b}$$

$$\begin{pmatrix}\boldsymbol{M}_{\substack{e\\o}m+1,n}^{+(i)}(c,\xi)\\ \boldsymbol{N}_{\substack{e\\o}m+1,n}^{+(i)}(c,\xi)\end{pmatrix}=\frac{1}{2}\left[\begin{pmatrix}\boldsymbol{M}_{\substack{e\\o}mn}^{x(i)}(c,\xi)\\ \boldsymbol{N}_{\substack{e\\o}mn}^{x(i)}(c,\xi)\end{pmatrix}\mp\begin{pmatrix}\boldsymbol{M}_{\substack{o\\e}mn}^{y(i)}(c,\xi)\\ \boldsymbol{N}_{\substack{o\\e}mn}^{y(i)}(c,\xi)\end{pmatrix}\right], \tag{4a}$$

$$\begin{pmatrix}\boldsymbol{M}_{\substack{e\\o}m-1,n}^{-(i)}(c,\xi)\\ \boldsymbol{N}_{\substack{e\\o}m-1,n}^{-(i)}(c,\xi)\end{pmatrix}=\frac{1}{2}\left[\begin{pmatrix}\boldsymbol{M}_{\substack{e\\o}mn}^{x(i)}(c,\xi)\\ \boldsymbol{N}_{\substack{e\\o}mn}^{x(i)}(c,\xi)\end{pmatrix}\pm\begin{pmatrix}\boldsymbol{M}_{\substack{o\\e}mn}^{y(i)}(c,\xi)\\ \boldsymbol{N}_{\substack{o\\e}mn}^{y(i)}(c,\xi)\end{pmatrix}\right], \tag{4b}$$

where $S_{mn}(c,\eta)$ and $R_{mn}^{(i)}(c,\xi)$ stand for the angular function and the radial function of the i-th kind, respectively. It is worth noting that in the limit when the focal distance d becomes zero or the ξ approaches infinity (η =constant), $S_{mn}(c,\eta)$ and $R_{mn}^{(i)}(c,\xi)$ reduce to the Legendre and Bessel functions in the spherical system, respectively.

The unknown coefficients $A_{\substack{e\\o}mn}^{(z,\pm)M}$, $A_{\substack{e\\o}mn}^{(z,\pm)N}$, $B_{\substack{e\\o}mn}^{(z,\pm)M}$ and $B_{\substack{e\\o}mn}^{(z,\pm)N}$ can be solved by substituting (1a) and (1b) into the following boundary conditions at the spheroidal interface $\xi = \xi_0$:

$$\hat{\boldsymbol{\xi}} \times \boldsymbol{E}_I = \hat{\boldsymbol{\xi}} \times \boldsymbol{E}_{II}, \tag{5a}$$

$$\frac{1}{\mu_1}\hat{\boldsymbol{\xi}} \times \boldsymbol{\nabla} \times \boldsymbol{E}_I = \frac{1}{\mu_2}\hat{\boldsymbol{\xi}} \times \boldsymbol{\nabla} \times \boldsymbol{E}_{II}, \tag{5b}$$

where the magnetic permeabilities of the two regions are assumed as $\mu_1 = \mu_2 = \mu_0$, and the following relations are used:

$$\boldsymbol{\nabla} \times \boldsymbol{M}_{\substack{e\\o}mn}^{z(i),\pm(i)}(c,\xi) = k\boldsymbol{N}_{\substack{e\\o}mn}^{z(i),\pm(i)}(c,\xi), \tag{6a}$$

$$\boldsymbol{\nabla} \times \boldsymbol{N}_{\substack{e\\o}mn}^{z(i),\pm(i)}(c,\xi) = k\boldsymbol{M}_{\substack{e\\o}mn}^{z(i),\pm(i)}(c,\xi). \tag{6b}$$

2.3 Determination of Unknown Coefficients

Because of the orthogonality of the trigonometric functions, the coefficients of the same ϕ-dependent trigonometric function in (5a) and (5b) must be equal, component by component; the equalities must hold for each corresponding term in the summation over m. For the summation over n, however, the individual terms in the series cannot be decomposed term by term. This causes the difficulty in determining the unknown coefficients. To solve for the unknown coefficients, the following expanded intermediate forms [22, 36, 37] are introduced:

$$\sum_{t=0}^{\infty} I_{t,1}^{mn}(c) \cdot P_{m-1+t}^{m-1}(\eta) = (1-\eta^2)^{-1/2}\mathcal{S}_n^m(c,\eta), \tag{7a}$$

$$\sum_{t=0}^{\infty} I_{t,2}^{mn}(c) \cdot P_{m-1+t}^{m-1}(\eta) = (1-\eta^2)^{1/2}\mathcal{S}_n^m(c,\eta), \tag{7b}$$

$$\sum_{t=0}^{\infty} I_{t,3}^{mn}(c) \cdot P_{m-1+t}^{m-1}(\eta) = (1-\eta^2)^{3/2}\mathcal{S}_n^m(c,\eta), \tag{7c}$$

$$\sum_{t=0}^{\infty} I_{t,4}^{mn}(c) \cdot P_{m-1+t}^{m-1}(\eta) = (1-\eta^2)^{5/2}\mathcal{S}_n^m(c,\eta), \tag{7d}$$

$$\sum_{t=0}^{\infty} I_{t,5}^{mn}(c) \cdot P_{m-1+t}^{m-1}(\eta) = \eta(1-\eta^2)^{-1/2}\mathcal{S}_n^m(c,\eta), \tag{7e}$$

$$\sum_{t=0}^{\infty} I_{t,6}^{mn}(c)\cdot P_{m-1+t}^{m-1}(\eta)=\eta(1-\eta^2)^{1/2}\mathcal{S}_n^m(c,\eta), \tag{7f}$$

$$\sum_{t=0}^{\infty} I_{t,7}^{mn}(c)\cdot P_{m-1+t}^{m-1}(\eta)=\eta(1-\eta^2)^{3/2}\mathcal{S}_n^m(c,\eta), \tag{7g}$$

$$\sum_{t=0}^{\infty} I_{t,8}^{mn}(c)\cdot P_{m-1+t}^{m-1}(\eta)=(1-\eta^2)^{1/2}\frac{d\mathcal{S}_n^m(c,\eta)}{d\eta}, \tag{7h}$$

$$\sum_{t=0}^{\infty} I_{t,9}^{mn}(c)\cdot P_{m-1+t}^{m-1}(\eta)=(1-\eta^2)^{3/2}\frac{d\mathcal{S}_n^m(c,\eta)}{d\eta}, \tag{7i}$$

$$\sum_{t=0}^{\infty} I_{t,10}^{mn}(c)\cdot P_{m-1+t}^{m-1}(\eta)=(1-\eta^2)^{5/2}\frac{d\mathcal{S}_n^m(c,\eta)}{d\eta}, \tag{7j}$$

$$\sum_{t=0}^{\infty} I_{t,11}^{mn}(c)\cdot P_{m-1+t}^{m-1}(\eta)=\eta(1-\eta^2)^{1/2}\frac{d\mathcal{S}_n^m(c,\eta)}{d\eta}, \tag{7k}$$

$$\sum_{t=0}^{\infty} I_{t,12}^{mn}(c)\cdot P_{m-1+t}^{m-1}(\eta)=\eta(1-\eta^2)^{3/2}\frac{d\mathcal{S}_n^m(c,\eta)}{d\eta}, \tag{7l}$$

and

$$\sum_{t=0}^{\infty} I_{t,2}^{0n}(c)\cdot P_{1+t}^{1}(\eta)=(1-\eta^2)^{1/2}\mathcal{S}_n^0(c,\eta), \tag{8a}$$

$$\sum_{t=0}^{\infty} I_{t,3}^{0n}(c)\cdot P_{1+t}^{1}(\eta)=(1-\eta^2)^{3/2}\mathcal{S}_n^0(c,\eta), \tag{8b}$$

$$\sum_{t=0}^{\infty} I_{t,4}^{0n}(c)\cdot P_{1+t}^{1}(\eta)=(1-\eta^2)^{5/2}\mathcal{S}_n^0(c,\eta), \tag{8c}$$

$$\sum_{t=0}^{\infty} I_{t,6}^{0n}(c)\cdot P_{1+t}^{1}(\eta)=\eta(1-\eta^2)^{1/2}\mathcal{S}_n^0(c,\eta), \tag{8d}$$

$$\sum_{t=0}^{\infty} I_{t,7}^{0n}(c)\cdot P_{1+t}^{1}(\eta)=\eta(1-\eta^2)^{3/2}\mathcal{S}_n^0(c,\eta), \tag{8e}$$

$$\sum_{t=0}^{\infty} I_{t,8}^{0n}(c)\cdot P_{1+t}^{1}(\eta)=(1-\eta^2)^{1/2}\frac{d\mathcal{S}_n^0(c,\eta)}{d\eta}, \tag{8f}$$

$$\sum_{t=0}^{\infty} I_{t,9}^{0n}(c)\cdot P_{1+t}^{1}(\eta)=(1-\eta^2)^{3/2}\frac{d\mathcal{S}_n^0(c,\eta)}{d\eta}, \tag{8g}$$

$$\sum_{t=0}^{\infty} I_{t,10}^{0n}(c)\cdot P_{1+t}^{1}(\eta)=(1-\eta^2)^{5/2}\frac{d\mathcal{S}_n^0(c,\eta)}{d\eta}, \tag{8h}$$

$$\sum_{t=0}^{\infty} I_{t,11}^{0n}(c)\cdot P_{1+t}^{1}(\eta)=\eta(1-\eta^2)^{1/2}\frac{d\mathcal{S}_n^0(c,\eta)}{d\eta}, \tag{8i}$$

$$\sum_{t=0}^{\infty} I_{t,12}^{0n}(c)\cdot P_{1+t}^{1}(\eta)=\eta(1-\eta^2)^{3/2}\frac{d\mathcal{S}_n^0(c,\eta)}{d\eta}, \tag{8j}$$

where the intermediates $I_{t,\ell}^{mn}$ ($t=0,1,2,\cdots$ and $\ell=1,2,\cdots,12$) have been provided in closed form in the Appendix A. The individual terms in the summation over t must be matched term by term, by considering the orthogonality of the associated Legendre functions $P_{m-1+t}^{m-1}(\eta)$. By substitution of the above equations, all factors that are functions of η are replaced by a series of the associated Legendre functions, which are orthogonal functions in the interval $-1\le\eta\le 1$. Thus, the equations used to determine the unknown coefficients constitute an infinite system of coupled linear equations as follows:

$$\sum_{n=m}^{\infty}\Gamma_{mn}^{z}\cdot\begin{pmatrix} \mp\mathcal{U}_{\substack{o\\e}mn\theta}^{z(1),t}(c_1) & \mathcal{V}_{\substack{e\\o}mn\theta}^{z(1),t}(c_1) & \pm\mathcal{U}_{\substack{o\\e}mn\theta}^{z(3),t}(c_2) & -\mathcal{V}_{\substack{e\\o}mn\theta}^{z(3),t}(c_2)\\ \mathcal{U}_{\substack{o\\e}mn\phi}^{z(1),t}(c_1) & \mp\mathcal{V}_{\substack{e\\o}mn\phi}^{z(1),t}(c_1) & -\mathcal{U}_{\substack{o\\e}mn\phi}^{z(3),t}(c_2) & \pm\mathcal{V}_{\substack{e\\o}mn\phi}^{z(3),t}(c_2)\\ \mathcal{V}_{\substack{o\\e}mn\theta}^{z(1),t}(c_1) & \pm\mathcal{U}_{\substack{e\\o}mn\theta}^{z(1),t}(c_1) & -\rho\mathcal{V}_{\substack{o\\e}mn\theta}^{z(3),t}(c_2) & \mp\rho\mathcal{U}_{\substack{e\\o}mn\theta}^{z(3),t}(c_2)\\ \pm\mathcal{V}_{\substack{o\\e}mn\phi}^{z(1),t}(c_1) & \mathcal{U}_{\substack{e\\o}mn\phi}^{z(1),t}(c_1) & \mp\rho\mathcal{V}_{\substack{o\\e}mn\phi}^{z(3),t}(c_2) & -\rho\mathcal{U}_{\substack{e\\o}mn\phi}^{z(3),t}(c_2) \end{pmatrix}$$
$$\cdot\begin{pmatrix} A_{\substack{o\\e}mn}^{zM}\\ A_{\substack{e\\o}mn}^{zN}\\ B_{\substack{o\\e}mn}^{zM}\\ B_{\substack{e\\o}mn}^{zN}\end{pmatrix}=\sum_{n=m}^{\infty}\Gamma_{mn}^{z}\cdot\begin{pmatrix} \mathcal{V}_{\substack{e\\o}mn\theta}^{z(1),t}(c_2)\\ \mp\mathcal{V}_{\substack{e\\o}mn\phi}^{z(1),t}(c_2)\\ \pm\rho\mathcal{U}_{\substack{e\\o}mn\theta}^{z(1),t}(c_2)\\ \rho\mathcal{U}_{\substack{e\\o}mn\phi}^{z(1),t}(c_2)\end{pmatrix}, \tag{9a}$$

$$\sum_{n=m}^{\infty}\Gamma_{mn}^{y}\cdot\begin{pmatrix} \mp\mathcal{U}_{\substack{e\\o}mn\theta}^{+(1),t}(c_1) & \mathcal{V}_{\substack{o\\e}mn\theta}^{+(1),t}(c_1) & \pm\mathcal{U}_{\substack{e\\o}mn\theta}^{+(3),t}(c_2) & -\mathcal{V}_{\substack{o\\e}mn\theta}^{+(3),t}(c_2)\\ \mathcal{U}_{\substack{e\\o}mn\phi}^{+(1),t}(c_1) & \mp\mathcal{V}_{\substack{o\\e}mn\phi}^{+(1),t}(c_1) & -\mathcal{U}_{\substack{e\\o}mn\phi}^{+(3),t}(c_2) & \pm\mathcal{V}_{\substack{o\\e}mn\phi}^{+(3),t}(c_2)\\ \mathcal{V}_{\substack{e\\o}mn\theta}^{+(1),t}(c_1) & \pm\mathcal{U}_{\substack{o\\e}mn\theta}^{+(1),t}(c_1) & -\rho\mathcal{V}_{\substack{e\\o}mn\theta}^{+(3),t}(c_2) & \mp\rho\mathcal{U}_{\substack{o\\e}mn\theta}^{+(3),t}(c_2)\\ \pm\mathcal{V}_{\substack{e\\o}mn\phi}^{+(1),t}(c_1) & \mathcal{U}_{\substack{o\\e}mn\phi}^{+(1),t}(c_1) & \mp\rho\mathcal{V}_{\substack{e\\o}mn\phi}^{+(3),t}(c_2) & -\rho\mathcal{U}_{\substack{o\\e}mn\phi}^{+(3),t}(c_2) \end{pmatrix}$$

$$\cdot \begin{pmatrix} A_{e\,o^{mn}}^{+yM} \\ A_{o\,e^{mn}}^{+yN} \\ B_{e\,o^{mn}}^{+yM} \\ B_{o\,e^{mn}}^{+yN} \end{pmatrix} = \sum_{n=m}^{\infty} \Gamma_{mn}^{y} \cdot \begin{pmatrix} \pm \mathcal{V}_{e\,o^{mn\theta}}^{+(1),t}(c_2) \\ -\mathcal{V}_{o\,e^{mn\phi}}^{+(1),t}(c_2) \\ \rho \mathcal{U}_{e\,o^{mn\theta}}^{+(1),t}(c_2) \\ \pm \rho \mathcal{U}_{o\,e^{mn\phi}}^{+(1),t}(c_2) \end{pmatrix}, \tag{9b}$$

$$\sum_{n=m}^{\infty} \Gamma_{mn}^{y} \cdot \begin{pmatrix} \pm \mathcal{U}_{e\,o^{mn\theta}}^{-(1),t}(c_1) & \mathcal{V}_{o\,e^{mn\theta}}^{-(1),t}(c_1) & \mp \mathcal{U}_{e\,o^{mn\theta}}^{-(3),t}(c_2) & -\mathcal{V}_{o\,e^{mn\theta}}^{-(3),t}(c_2) \\ \mathcal{U}_{e\,o^{mn\phi}}^{-(1),t}(c_1) & \pm \mathcal{V}_{o\,e^{mn\phi}}^{-(1),t}(c_1) & -\mathcal{U}_{e\,o^{mn\phi}}^{-(3),t}(c_2) & \mp \mathcal{V}_{o\,e^{mn\phi}}^{-(3),t}(c_2) \\ \mathcal{V}_{e\,o^{mn\theta}}^{-(1),t}(c_1) & \mp \mathcal{U}_{o\,e^{mn\theta}}^{+(1),t}(c_1) & -\rho \mathcal{V}_{e\,o^{mn\theta}}^{-(3),t}(c_2) & \pm \rho \mathcal{U}_{o\,e^{mn\theta}}^{-(3),t}(c_2) \\ \mp \mathcal{V}_{e\,o^{mn\phi}}^{-(1),t}(c_1) & \mathcal{U}_{o\,e^{mn\phi}}^{-(1),t}(c_1) & \pm \rho \mathcal{V}_{e\,o^{mn\phi}}^{-(3),t}(c_2) & -\rho \mathcal{U}_{o\,e^{mn\phi}}^{-(3),t}(c_2) \end{pmatrix}$$

$$\cdot \begin{pmatrix} A_{e\,o^{mn}}^{-yM} \\ A_{o\,e^{mn}}^{-yN} \\ B_{e\,o^{mn}}^{-yM} \\ B_{o\,e^{mn}}^{-yN} \end{pmatrix} = \sum_{n=m}^{\infty} \Gamma_{mn}^{y} \cdot \begin{pmatrix} \mp \mathcal{V}_{e\,o^{mn\theta}}^{-(1),t}(c_2) \\ -\mathcal{V}_{o\,e^{mn\phi}}^{-(1),t}(c_2) \\ \rho \mathcal{U}_{e\,o^{mn\theta}}^{-(1),t}(c_2) \\ \mp \rho \mathcal{U}_{o\,e^{mn\phi}}^{-(1),t}(c_2) \end{pmatrix}, \tag{9c}$$

where the ratio ρ denotes the value of $\sqrt{\epsilon_2/\epsilon_1}$. Γ_{mn}^{z} and Γ_{mn}^{y} are

$$\iiint_{V'} \frac{2-\delta_{m0}}{N_{mn}} \psi_{e\,o^{mn}}^{(3)}(k_2, \xi') I_z(\xi') dV'$$

and

$$\iiint_{V'} \frac{2-\delta_{m0}}{N_{mn}} \psi_{e\,o^{mn}}^{(3)}(k_2, \xi') I_y(\xi') dV'$$

in values, respectively. Details of $\mathcal{U}_{e\,o^{mn\theta}}^{q(i),t}$, $\mathcal{U}_{e\,o^{mn\phi}}^{q(i),t}$, $\mathcal{V}_{e\,o^{mn\theta}}^{q(i),t}$, and $\mathcal{V}_{e\,o^{mn\phi}}^{q(i),t}$ ($q = z, \pm$, and $i = 1, 2$) are given in the Appendix B.

In principle, by making t sufficiently large an adequate number of relations satisfied by unknown coefficients are formulated and the unknown coefficients can be solved for uniquely.

3. NUMERICAL COMPUTATION AND RESULTS

3.1 Numerical Computation

The tabulated numerical values of the angular and radial functions in the spheroidal coordinate system that have been published to date are not enough, particularly, for large and complex values of c [38–40]. The Mathematica^{TM} package capable of calculating the angular and radial functions with large c values and complex arguments has been developed in [40]. This package has been used in this paper in order to obtain more accurate values of the angular and radial harmonics and the scattering coefficients of the electromagnetic fields. Practically, a system of infinite equations is truncated to a finite number of equations, i.e., the same number of unknowns. The standard numerical techniques for matrix manipulations are employed at a specified accuracy of relative error 0.1%. Finally, the specific absorption rate (SAR), which quantifies the power absorbed per unit mass of tissue, is calculated. SAR is defined as $\sigma|\boldsymbol{E}|^2/2\rho$, where σ and ρ represent the average conductivity and density ($\cong$ 1050 kg/m^3) of the human head model, respectively. To simplify the calculation, the transmitted power of the dipole is assumed to be 1 watt at both the GSM and PCN frequencies.

3.2 Results and Discussion

The various SAR distributions inside the prolate spheroidal human head model for GSM and PCN dipoles are calculated and the results are shown in Fig. 2–Fig. 9. The inner SAR distributions of the spherical human head model are depicted in Fig. 10 and Fig. 11 for comparisons. The peak SAR values in the human head models vary with the inclination and location of the dipole; such variations in various cases are also illustrated in Fig. 12 and Fig. 13. In all these figures, the dipole is placed on the right of the model and the SAR values for each figure are normalized to the peak value of SAR in the model.

The EM field distribution inside the spheroidal head model for a GSM dipole differs from that for a PCN dipole, as shown in Fig. 2 and Fig. 3. It is also seen that the inner field due to the PCN dipole exhibits an obvious resonant effect and the normalized peak value is smaller than that of its GSM counterpart. This is because the dimension of

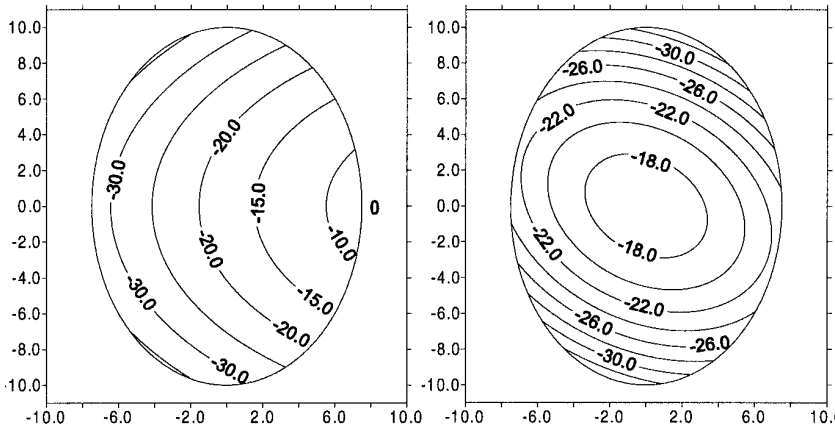

(a) $\phi = 0$ and π (rear view) (b) $\phi = \pi/2$ and $3\pi/2$ (side view)

Figure 2. SAR distributions (in dB) of the prolate spheroidal head model ($\frac{\lambda}{4}$ GSM dipole), normalized to 3.38 W/kg. $s = 1.5$ cm, $\beta = 30°$, the unit of the coordinate is in cm.

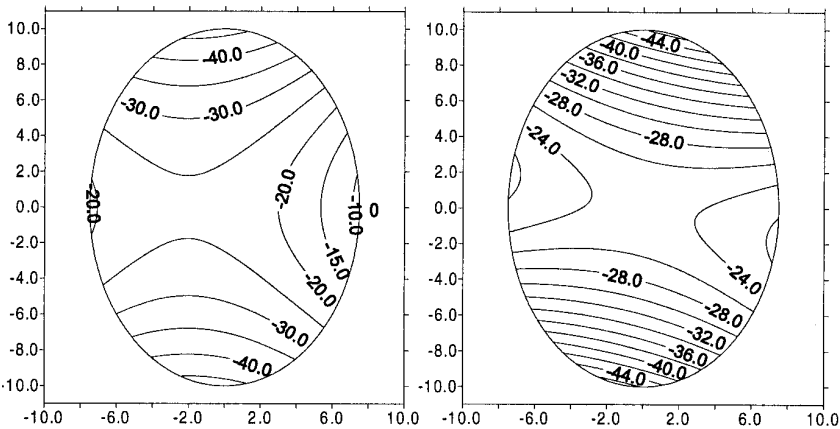

(a) $\phi = 0$ and π (rear view) (b) $\phi = \pi/2$ and $3\pi/2$ (side view)

Figure 3. SAR distributions (in dB) of the prolate spheroidal head model ($\frac{\lambda}{4}$ PCN dipole), normalized to 1.02 W/kg. $s = 1.5$ cm, $\beta = 30°$, the unit of the coordinate is in cm.

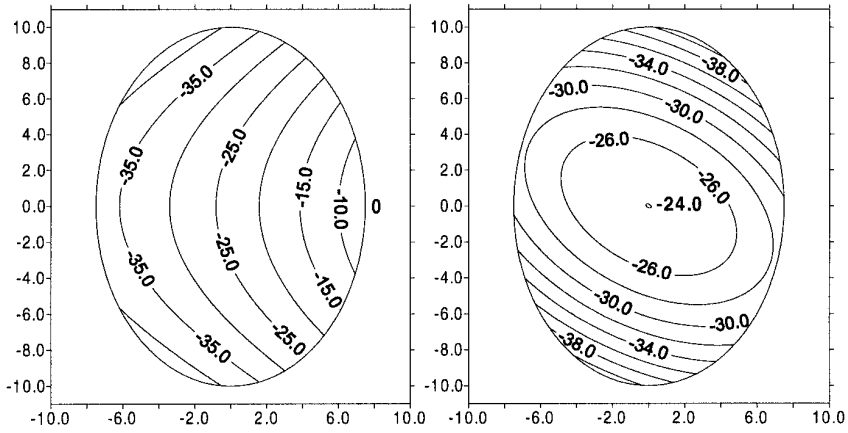

(a) $\phi = 0$ and π (rear view) (b) $\phi = \pi/2$ and $3\pi/2$ (side view)

Figure 4. SAR distributions (in dB) of the prolate spheroidal head model ($\frac{\lambda}{4}$ GSM dipole), normalized to 6.08 W/kg. $s = 0.75$ cm, $\beta = 30°$, the unit of the coordinate is in cm.

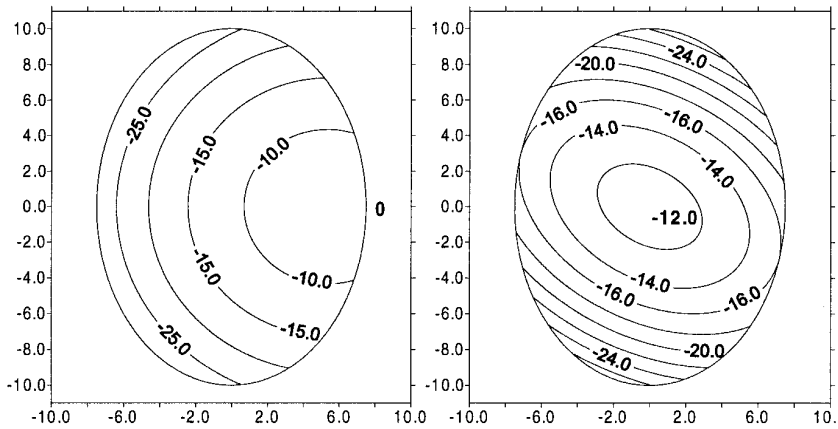

(a) $\phi = 0$ and π (rear view) (b) $\phi = \pi/2$ and $3\pi/2$ (side view)

Figure 5. SAR distributions (in dB) of the prolate spheroidal head model ($\frac{\lambda}{4}$ GSM dipole), normalized to 1.16 W/kg. $s = 2.5$ cm, $\beta = 30°$, the unit of the coordinate is in cm.

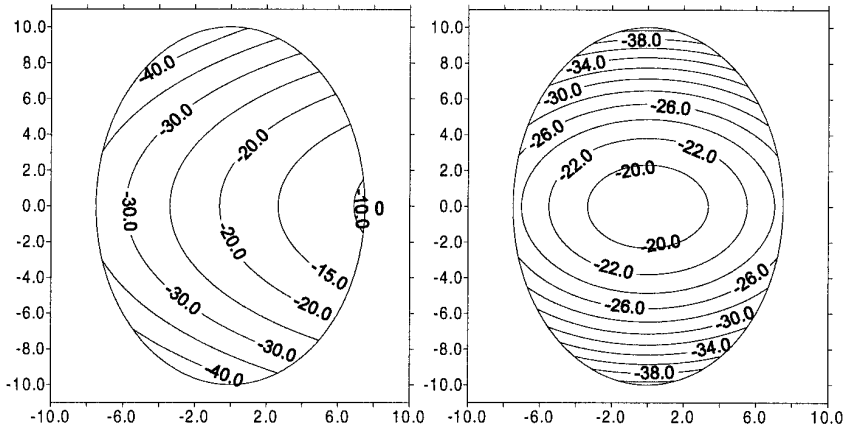

(a) $\phi = 0$ and π (rear view) (b) $\phi = \pi/2$ and $3\pi/2$ (side view)

Figure 6. SAR distributions (in dB) of the prolate spheroidal head model ($\frac{\lambda}{4}$ GSM dipole), normalized to 2.89 W/kg. $s = 1.5$ cm, $\beta = 0°$, the unit of the coordinate is in cm.

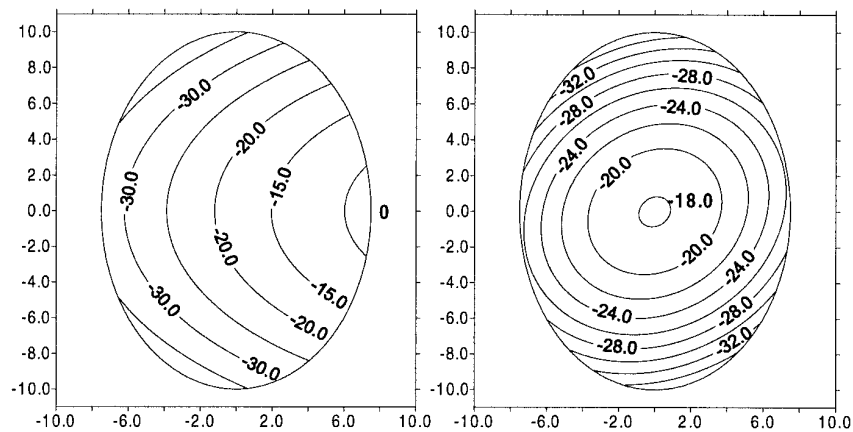

(a) $\phi = 0$ and π (rear view) (b) $\phi = \pi/2$ and $3\pi/2$ (side view)

Figure 7. SAR distributions (in dB) of the prolate spheroidal head model ($\frac{\lambda}{4}$ GSM dipole), normalized to 5.39 W/kg. $s = 1.5$ cm, $\beta = 60°$, the unit of the coordinate is in cm.

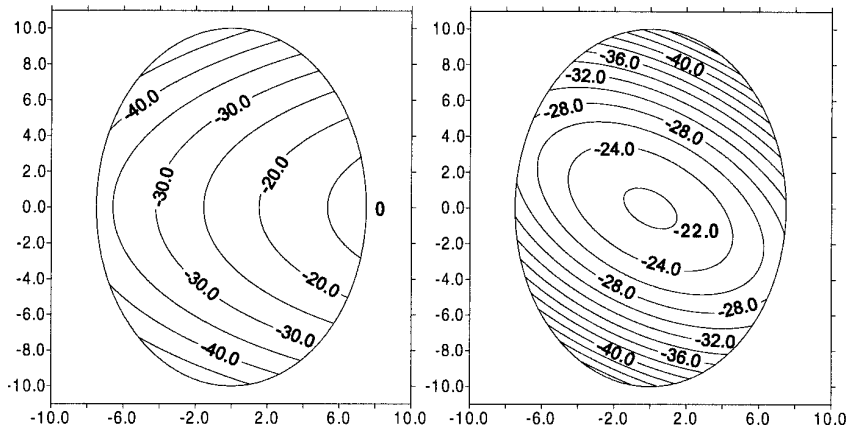

(a) $\phi = 0$ and π (rear view) (b) $\phi = \pi/2$ and $3\pi/2$ (side view)

Figure 8. SAR distributions (in dB) of the prolate spheroidal head model (GSM small dipole), normalized to 6.18 W/kg. $s = 1.5$ cm, $\beta = 30^\circ$, the unit of the coordinate is in cm.

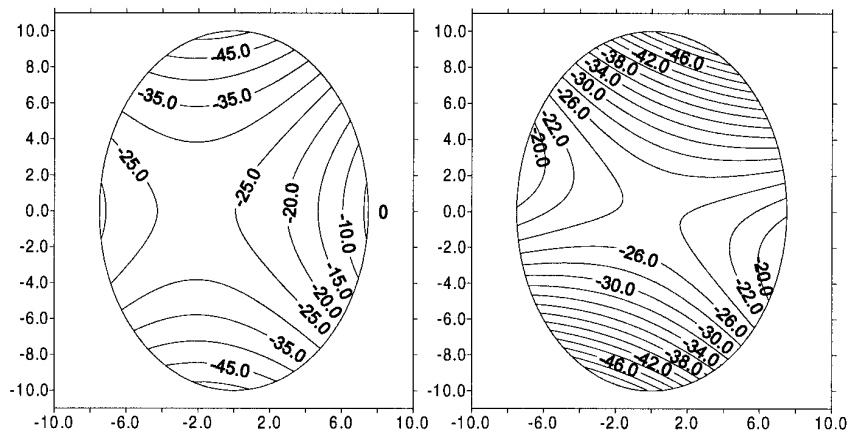

(a) $\phi = 0$ and π (rear view) (b) $\phi = \pi/2$ and $3\pi/2$ (side view)

Figure 9. SAR distributions (in dB) of the prolate spheroidal head model (PCN small dipole), normalized to 2.49 W/kg. $s = 1.5$ cm, $\beta = 30^\circ$, the unit of the coordinate is in cm.

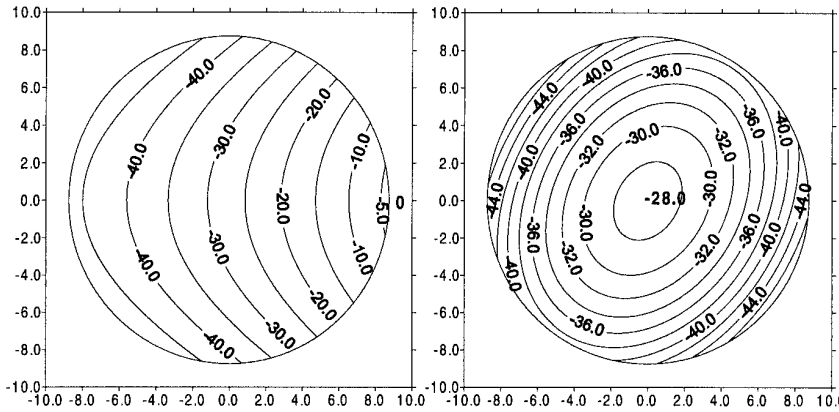

(a) $\phi = 0$ and π (rear view) (b) $\phi = \pi/2$ and $3\pi/2$ (side view)

Figure 10. SAR distributions (in dB) of the spherical head model ($\frac{\lambda}{4}$ GSM dipole), normalized to 3.43 W/kg. $s = 1.5$ cm, $\beta = 30°$, the unit of the coordinate is in cm.

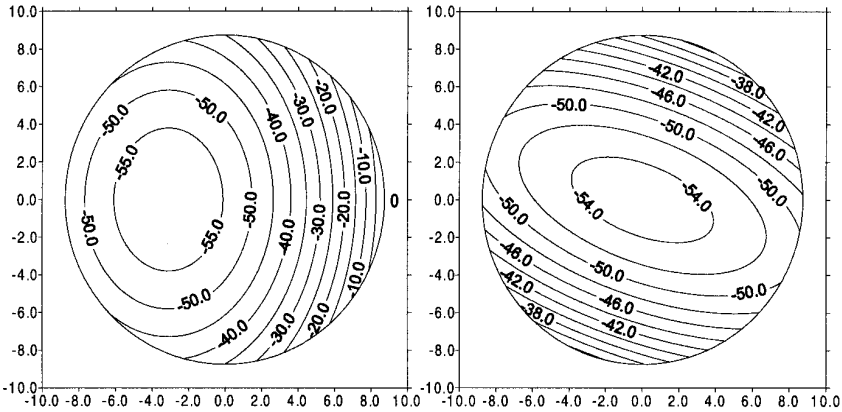

(a) $\phi = 0$ and π (rear view) (b) $\phi = \pi/2$ and $3\pi/2$ (side view)

Figure 11. SAR distributions (in dB) of the spherical head model ($\frac{\lambda}{4}$ PCN dipole), normalized to 1.64 W/kg. $s = 1.5$ cm, $\beta = 30°$, the unit of the coordinate is in cm.

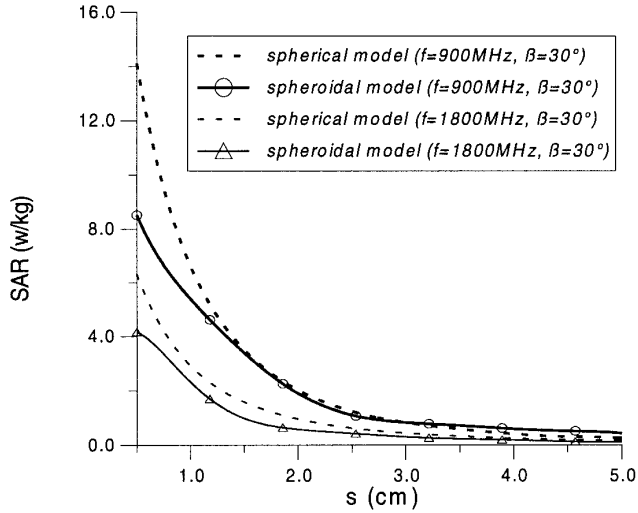

Figure 12. Peak SAR value versus s and f (spheroidal and spherical models).

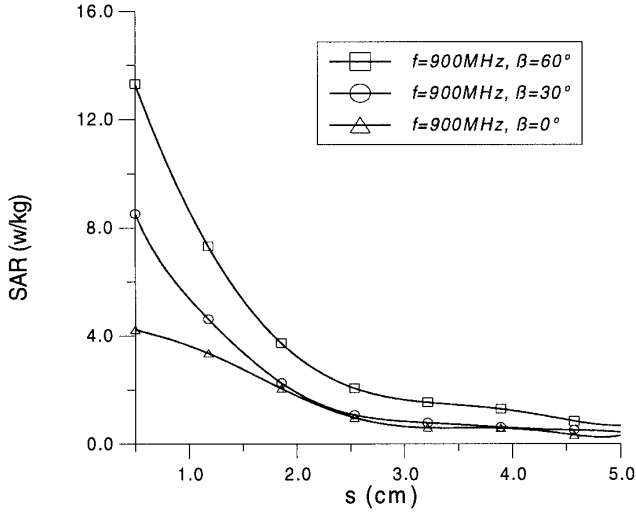

Figure 13. Peak SAR value versus s and β (prolate spheroidal model).

the head model is close to the PCN antenna wavelength (about 17 cm). This fundamental and important aspect of the overall interaction of microwaves with biological objects possessing a closed surface area or containing a finite volume has been illustrated using spherical models by many other authors [12, 14, 15]. In contrast to that of the spherical model (as shown in Fig. 10 and Fig. 11), the cross sectional SARs around the two poles of the spheroidal model (Fig. 2(b) and Fig. 3(b)) are much lower. It is apparent that there exist obvious differences in the inner field distributions between the prolate spheroidal head model and the spherical head model.

It is found that the EM field inside the head model is more concentrated around the central part (near the right ear and temple), but the peak value decreases when the distance between the head and the dipole becomes larger (as shown in Fig. 2(a), Fig. 4(a), and Fig. 5(a)). The SAR distributions in the cross section of the head in Fig. 2(b), Fig. 4(b), and Fig. 5(b) (side view) are similar for various distance s, but the corresponding value decreases when the s increases. The EM field distributions at the GSM frequency at different inclination angles of the dipole exhibit a similar attenuation rate along the direction of wave propagation, except that the peak value of SAR increases with the inclination angle (as illustrated in Fig. 2(a), Fig. 6(a), and Fig. 7(a)). Apparently, there are somewhat changes of the cross sectional SAR distributions due to the different inclination angles β of the dipole (shown in profiles of Fig. 2(b), Fig. 6(b), and Fig. 7(b)).

The results of the inner SAR distributions for $\lambda/4$ dipoles and small dipoles at the same frequencies are similar but the normalized peak values for the small dipoles are larger (shown in Fig. 2, Fig. 3, Fig. 8 and Fig. 9). This is due to less radiation resistance of the small dipole antenna (the radiation power is assumed to be unchanged).

From Fig. 12 and Fig. 13, it is clear that the peak SAR values in all the cases decay fast when the distance between the dipole and the head model becomes larger. For the spheroidal model at the GSM frequency, the peak value of SAR is much smaller than its spherical counterpart when the distance s is less than 1 cm, but the value is a bit higher when $s > 3$ cm. For the PCN dipole, the peak value of SAR of the spheroidal model is always smaller than its spherical counterpart. The peak SAR value increases with the inclination angle of the dipole and such a difference is illustrated larger when the distance s becomes smaller (shown in Fig. 13).

4. CONCLUSIONS

The EM field distributions inside a dielectric prolate spheroidal human head model are calculated using spheroidal vector wave functions and the coupled unknown coefficients are obtained numerically. The final results of the internal SAR distributions in various cases are presented. It is apparent that significant differences in the inner field distribution do exist between the prolate spheroidal head model and the spherical head model. In view of the fact that the human head should be better approximated by a prolate spheroid than a simple sphere, the full-wave analysis of the EM field distribution inside the human head using the prolate spheroidal model is more accurate and relevant to the actual case than that using the simple spherical model.

APPENDIX A: INTERMEDIATES $I_{t,\ell}^{mn}$ IN CLOSED FORM

A.1 The Case: $m \geq 1$

In the case $m \geq 1$, the intermediates in closed form are expressed as follows for odd $(n-m)+t$:

$$I_{t,1}^{mn} = I_{t,2}^{mn} = I_{t,3}^{mn} = I_{t,4}^{mn} = I_{t,11}^{mn} = I_{t,12}^{mn} = 0, \tag{A-1a}$$

$$\begin{aligned} I_{t,5}^{mn} &= [\mathcal{N}_1]^{-1} \int_{-1}^{+1} \eta(1-\eta^2)^{-1/2} \mathcal{S}_{m+r}^{m}(c,\eta) P_{m-1+t}^{m-1}(\eta) d\eta \\ &= t d_{t-1}^{mn} + (2t+2m-1) \sum_{r=t+1}^{\infty}{}' d_r^{mn}, \end{aligned} \tag{A-1b}$$

$$\begin{aligned} I_{t,6}^{mn} &= [\mathcal{N}_1]^{-1} \int_{-1}^{+1} \eta(1-\eta^2)^{1/2} \mathcal{S}_{m+r}^{m}(c,\eta) P_{m-1+t}^{m-1}(\eta) d\eta \\ &= \frac{(t+2m-1)(t+2m)}{(2t+2m+1)} \cdot \left[\frac{(t+2m+1)}{(2t+2m+3)} d_{t+1}^{mn} + \frac{t \cdot d_{t-1}^{mn}}{(2t+2m-1)} \right] \\ &\quad - \frac{t(t-1)}{(2t+2m-3)} \cdot \left[\frac{(t+2m-1)}{(2t+2m-1)} d_{t-1}^{mn} + \frac{(t-2)}{(2t+2m-5)} d_{t-3}^{mn} \right], \end{aligned} \tag{A-1c}$$

$$
\begin{aligned}
I_{t,7}^{mn} &= [\mathcal{N}_1]^{-1} \int_{-1}^{+1} \eta(1-\eta^2)^{3/2} \mathcal{S}_{m+r}^{m}(c,\eta) P_{m-1+t}^{m-1}(\eta) d\eta \\
&= \frac{(t+2m-1)(t+2m)(t+2m+1)(t+2m+2)(t+2m+3)}{(2t+2m+1)(2t+2m+3)(t+2m+5)} \\
&\quad \cdot \left[\frac{d_{t+1}^{mn}}{(2t+2m+3)} - \frac{d_{t+3}^{mn}}{(2t+2m+7)} \right] \\
&\quad - \frac{t(t-2m)(t+2m-1)(t+2m)(t+2m+1)}{(2t+2m-3)(2t+2m+1)(2t+2m+3)} \\
&\quad \cdot \left[\frac{d_{t-1}^{mn}}{(2t+2m-1)} - \frac{d_{t+1}^{mn}}{(2t+2m+3)} \right] \\
&\quad - \frac{t(t-1)(t-2)(t+2m-1)(t+4m-1)}{(2t+2m-5)(2t+2m-3)(2t+2m+1)} \cdot \left[\frac{d_{t-3}^{mn}}{(2t+2m-5)} \right. \\
&\quad \left. - \frac{d_{t-1}^{mn}}{(2t+2m-1)} \right] + \frac{t(t-1)(t-2)(t-3)(t-4)}{(2t+2m-7)(2t+2m-5)(2t+2m-3)} \\
&\quad \cdot \left[\frac{d_{t-5}^{mn}}{(2t+2m-9)} - \frac{d_{t-3}^{mn}}{(2t+2m-5)} \right], \qquad \text{(A-1d)} \\
I_{t,8}^{mn} &= [\mathcal{N}_1]^{-1} \int_{-1}^{+1} (1-\eta^2)^{1/2} \frac{d\mathcal{S}_{m+r}^{m}(c,\eta)}{d\eta} P_{m-1+t}^{m-1}(\eta) d\eta \\
&= -t(t+m-1) d_{t-1}^{mn} + m(2t+2m-1) \sum_{r=t+1}^{\infty}{}' d_r^{mn}, \qquad \text{(A-1e)} \\
I_{t,9}^{mn} &= [\mathcal{N}_1]^{-1} \int_{-1}^{+1} (1-\eta^2)^{3/2} \frac{d\mathcal{S}_{m+r}^{m}(c,\eta)}{d\eta} P_{m-1+t}^{m-1}(\eta) d\eta \\
&= \frac{(t+2m-1)(t+2m)}{(2t+2m+1)} \left[\frac{(t+m+2)(t+2m+1)}{(2t+2m+3)} d_{t+1}^{mn} \right. \\
&\quad \left. - \frac{t(m+t-1)}{(2t+2m-1)} d_{t-1}^{mn} \right] - \frac{t(t-1)}{(2t+2m-3)} \\
&\quad \cdot \left[\frac{(t+m)(t+2m-1)}{(2t+2m-1)} d_{t-1}^{mn} - \frac{(t-2)(t+m-3)}{(2t+2m-5)} d_{t-3}^{mn} \right], \qquad \text{(A-1f)}
\end{aligned}
$$

$$
\begin{aligned}
I_{t,10}^{mn} &= [\mathcal{N}_1]^{-1} \int_{-1}^{+1} (1-\eta^2)^{5/2} \frac{d\mathcal{S}_{m+r}^{m}(c,\eta)}{d\eta} P_{m-1+t}^{m-1}(\eta) d\eta \\
&= I_{t,9}^{mn} - \left\{ \frac{(t+2m-1)(t+2m)(t+2m+1)}{(2t+2m+1)(2t+2m+3)(2t+2m+5)} \right. \\
&\quad \cdot \left[\frac{(t+1)(t+2m+2)(t+2m+3)}{2(2t+2m+3)} d_{t+1}^{mn} \right. \\
&\quad + \frac{(t+2)(t+3)(t+2m+1)}{2(2t+2m+3)} d_{t+1}^{mn} \\
&\quad \left. + \frac{(t+2m+2)(t+2m+3)(t+m+4)}{(2t+2m+7)} d_{t+3}^{mn} \right] \\
&\quad - \frac{t(t-2m)(t+2m-1)}{(2t+2m-3)(2t+2m+1)(2t+2m+3)} \\
&\quad \cdot \left[\frac{t(t+1)(t+2m-1) + (t-1)(t+2m)(t+2m+1)}{2(2t+2m-1)} d_{t-1}^{mn} \right. \\
&\quad \left. + \frac{(t+2m)(t+2m+1)(t+m+2)}{(2t+2m+3)} d_{t+1}^{mn} \right] \Bigg\} \\
&\quad + \frac{m(t+2)(t+2m-1)(t+2m)(t+2m+1)}{(2t+2m+1)(2t+2m+3)^2} d_{t+1}^{mn} \\
&\quad + \frac{t(t-1)(t-2)(t+4m-1)(t+2m-1)(t+m)}{(t+2m-5)(2t+2m-3)(2t+2m-1)(2t+2m+1)} d_{t-1}^{mn} \\
&\quad + \frac{mt(t+2m-1)}{2t+2m+3} \cdot \left[\frac{t+1}{2t+2m+1} \right. \\
&\quad \left. - \frac{t(t-2m)}{(2t+2m-3)(2t+2m-1)} \right] \cdot d_{t-1}^{mn} \\
&\quad + \frac{t(t-1)(t-2)(t-3)(t+4m-1)(t+2m-1)}{2(2t+2m-3)(2t+2m+1)(2t+2m-5)^2} d_{t-3}^{mn} \\
&\quad - \frac{t(t-1)(t-2)}{(2t+2m-3)(2t+2m-5)^2} \cdot \left[\frac{(t-3)(t-4)(t+m-2)}{2t+2m-7} \right. \\
&\quad \left. + m(t-2) \right] d_{t-3}^{mn} + \frac{t(t-1)(t-2)(t+2m-3)}{(2t+2m-5)(2t+2m-3)(2t+2m+1)} \\
&\quad \cdot \left[\frac{(t-2)(t-1) + 4m(2m-1) + (t-2m-1)(2m+1)}{2(2t+2m-5)} \right] d_{t-3}^{mn} \\
&\quad - \frac{t(t-1)(t-2)(t-3)(t-4)(t+m-5)}{(2t+2m-9)(2t+2m-7)(2t+2m-5)(2t+2m-3)} d_{t-5}^{mn},
\end{aligned}
\tag{A-1g}
$$

and for even $(n-m)+t$:

$$I_{t,5}^{mn} = I_{t,6}^{mn} = I_{t,7}^{mn} = I_{t,8}^{mn} = I_{t,9}^{mn} = I_{t,10}^{mn} = 0, \tag{A-2a}$$

$$\begin{aligned} I_{t,1}^{mn} &= [\mathcal{N}_1]^{-1} \int_{-1}^{+1} (1-\eta^2)^{-1/2} \mathcal{S}_{m+r}^{m}(c,\eta) P_{m-1+t}^{m-1}(\eta) d\eta \\ &= (2t+2m-1) \sum_{r=t}^{\infty} d_r^{mn}, \end{aligned} \tag{A-2b}$$

$$\begin{aligned} I_{t,2}^{mn} &= [\mathcal{N}_1]^{-1} \int_{-1}^{+1} (1-\eta^2)^{1/2} \mathcal{S}_{m+r}^{m}(c,\eta) P_{m-1+t}^{m-1}(\eta) d\eta \\ &= \frac{(t+2m-1)(t+2m)}{(2t+2m+1)} d_t^{mn} - \frac{t(t-1)}{(2t+2m-3)} d_{t-2}^{mn}, \end{aligned} \tag{A-2c}$$

$$\begin{aligned} I_{t,3}^{mn} &= [\mathcal{N}_1]^{-1} \int_{-1}^{+1} (1-\eta^2)^{3/2} \mathcal{S}_{m+r}^{m}(c,\eta) P_{m-1+t}^{m-1}(\eta) d\eta \\ &= \frac{(t+2m-1)(t+2m)(t+2m+1)(t+2m+2)}{(2t+2m+1)(2t+2m+3)} \\ &\quad \cdot \left[\frac{d_t^{mn}}{(2t+2m+1)} - \frac{d_{t+2}^{mn}}{(2t+2m+5)} \right] \\ &\quad - \frac{2t(t-1)(t+2m)(t+2m-1)}{(2t+2m-3)(2t+2m+1)} \cdot \left[\frac{d_{t-2}^{mn}}{(2t+2m-3)} \right. \\ &\quad \left. - \frac{d_t^{mn}}{(2t+2m+1)} \right] + \frac{t(t-1)(t-2)(t-3)}{(2t+2m-3)(2t+2m-5)} \\ &\quad \cdot \left[\frac{d_{t-4}^{mn}}{(2t+2m-7)} - \frac{d_{t-2}^{mn}}{(2t+2m-3)} \right], \end{aligned} \tag{A-2d}$$

$$\begin{aligned} I_{t,4}^{mn} &= [\mathcal{N}_1]^{-1} \int_{-1}^{+1} (1-\eta^2)^{5/2} \mathcal{S}_{m+r}^{m}(c,\eta) P_{m-1+t}^{m-1}(\eta) d\eta \\ &= I_{t,3}^{mn} - \left\{ \frac{(t+2m-1)(t+2m)(t+2m+1)(t+2m+2)}{(2t+2m+5)(2t+2m+1)} \right. \\ &\quad \cdot \frac{(t+2m+3)}{(2t+2m+3)} \left[\frac{(t+1)d_t^{mn}}{(2t+2m+1)(2t+2m+3)} \right. \\ &\quad \left. + \frac{(2m+1)d_{t+2}^{mn}}{(2t+2m+3)(2t+2m+7)} - \frac{(2m+t+4)d_{t+4}^{mn}}{(2t+2m+7)(2t+2m+9)} \right] \\ &\quad - \frac{t(t-2m)(t+2m-1)(t+2m)(t+2m+1)}{(2t+2m-3)(2t+2m+1)(2t+2m+3)} \\ &\quad \cdot \left[\frac{(t-1)d_{t-2}^{mn}}{(2t+2m-3)(2t+2m-1)} + \frac{(2m+1)d_t^{mn}}{(2t+2m-1)(2t+2m+3)} \right. \end{aligned}$$

$$
\begin{aligned}
&- \frac{(t+2m+2)d_{t+2}^{mn}}{(2t+2m+3)(2t+2m+5)}\Bigg] \\
&- \frac{t(t-1)(t-2)(t+2m-1)(t+4m-1)}{(2t+2m-5)(2t+2m-3)(2t+2m+1)} \\
&\cdot \left[\frac{(t-3)d_{t-4}^{mn}}{(2t+2m-7)(2t+2m-5)} + \frac{(2m+1)d_{t-2}^{mn}}{(2t+2m-5)(2t+2m-1)}\right. \\
&\left. - \frac{(2m+t)d_t^{mn}}{(2t+2m-1)(2t+2m+1)}\right] \\
&+ \frac{t(t-1)(t-2)(t-3)(t-4)}{(2t+2m-7)(2t+2m-5)(2t+2m-3)} \\
&\cdot \left[\frac{(t-5)d_{t-6}^{mn}}{(2t+2m-11)(2t+2m-9)} + \frac{(2m+1)d_{t-4}^{mn}}{(2t+2m-9)(2t+2m-5)}\right. \\
&\left. - \frac{(2m+t-2)d_{t-2}^{mn}}{(2t+2m-5)(2t+2m-3)}\right]\Bigg\}, \qquad \text{(A-2e)}
\end{aligned}
$$

$$
\begin{aligned}
I_{t,11}^{mn} &= [\mathcal{N}_1]^{-1}\int_{-1}^{+1}\eta(1-\eta^2)^{1/2}\frac{d\mathcal{S}_{m+r}^{m}(c,\eta)}{d\eta}P_{m-1+t}^{m-1}(\eta)d\eta \\
&= -\frac{t(t-1)(t+m-2)}{(2t+2m-3)}d_{t-2}^{mn} + m(2t+2m-1)\sum_{r=t+2}^{\infty}{}' d_r^{mn} \\
&\quad - \left[\frac{t(t-1)(2t+2m+1)}{2(2t+2m+1)} + \frac{(t+2m)(t+2m-1)}{2(2t+2m+1)}\right]d_t^{mn}, \qquad \text{(A-2f)}
\end{aligned}
$$

$$
\begin{aligned}
I_{t,12}^{mn} &= [\mathcal{N}_1]^{-1}\int_{-1}^{+1}\eta(1-\eta^2)^{3/2}\frac{d\mathcal{S}_{m+r}^{m}(c,\eta)}{d\eta}P_{m-1+t}^{m-1}(\eta)d\eta \\
&= \frac{(t+2m-1)(t+2m)}{(2t+2m+1)(2t+2m+3)}\cdot\left[\left(\frac{t(t+2m+1)(t+2m+2)}{2(2t+2m+1)}\right.\right. \\
&\quad \left.\left. + \frac{(t+1)(t+2)(t+2m)}{2(2t+2m+1)}\right)d_t^{mn}\right. \\
&\quad \left. + \frac{(t+m+3)(t+2m+1)(t+2m+2)}{(2t+2m+5)}d_{t+2}^{mn}\right] \\
&\quad - \frac{2t(t-1)}{(2t+2m-3)(2t+2m+1)}\cdot\left[\left(\frac{(t-2)(t+2m-1)(t+2m)}{2(2t+2m-3)}\right.\right. \\
&\quad \left.\left. + \frac{t(t-1)(t+2m-2)}{2(2t+2m-3)}\right)d_{t-2}^{mn}\right. \\
&\quad \left. + \frac{(t+m+1)(t+2m-1)(t+2m)}{(2t+2m+1)}d_t^{mn}\right]
\end{aligned}
$$

$$
\begin{aligned}
&+\frac{t(t-1)(t-2)(t-3)(t+m-1)}{(2t+2m-5)(2t+2m-3)^2}d_{t-2}^{mn}\\
&-\frac{m(t+1)(t+2m-1)(t+2m)}{(2t+2m+1)^2}d_t^{mn}\\
&-\frac{mt(t-1)}{(2t+2m+1)}\cdot\left[1-\frac{2(t-1)(2t+2m-1)}{(2t+2m-3)^2}\right]d_{t-2}^{mn}\\
&+\frac{t(t-1)(t-2)(t-3)(t+m-4)}{(2t+2m-7)(2t+2m-5)(2t+2m-3)}d_{t-4}^{mn}. \qquad \text{(A-2g)}
\end{aligned}
$$

A.2 The Case: $m = 0$

In the case $m = 0$, the intermediates reduce to the following formulas for odd $(n-m)+t$:

$$
I_{t,2}^{0n} = I_{t,3}^{0n} = I_{t,4}^{0n} = I_{t,11}^{0n} = I_{t,12}^{0n} = 0, \qquad \text{(A-3a)}
$$

$$
\begin{aligned}
I_{t,6}^{0n} &= [\mathcal{N}_2]^{-1}\int_{-1}^{+1}\eta(1-\eta^2)^{1/2}\mathcal{S}_r^0(c,\eta)P_{1+t}^1(\eta)d\eta\\
&= \frac{t+3}{2t+5}\left[\frac{d_{t+1}^{0n}}{2t+3}-\frac{d_{t+3}^{0n}}{2t+7}\right]+\frac{t}{2t+1}\left[\frac{d_{t-1}^{0n}}{2t-1}-\frac{d_{t+1}^{0n}}{2t+3}\right], \qquad \text{(A-3b)}
\end{aligned}
$$

$$
\begin{aligned}
I_{t,7}^{0n} &= [\mathcal{N}_2]^{-1}\int_{-1}^{+1}\eta(1-\eta^2)^{3/2}\mathcal{S}_r^0(c,\eta)P_{1+t}^1(\eta)d\eta\\
&= \frac{(t+3)(t+4)(t+5)}{(2t+5)(2t+7)}\\
&\quad\cdot\left[\frac{d_{t+1}^{0n}}{(2t+3)(2t+5)}-\frac{2d_{t+3}^{0n}}{(2t+5)(2t+9)}+\frac{d_{t+5}^{0n}}{(2t+9)(2t+11)}\right]\\
&\quad+\frac{3t(t+3)}{(2t+1)(2t+5)}\\
&\quad\cdot\left[\frac{d_{t-1}^{0n}}{(2t-1)(2t+1)}-\frac{2d_{t+1}^{0n}}{(2t+1)(2t+5)}+\frac{d_{t+3}^{0n}}{(2t+5)(2t+7)}\right]\\
&\quad-\frac{t(t-1)(t-2)}{(2t-1)(2t+1)}\\
&\quad\cdot\left[\frac{d_{t-3}^{0n}}{(2t-5)(2t-3)}-\frac{2d_{t-1}^{0n}}{(2t-3)(2t+1)}+\frac{d_{t+1}^{0n}}{(2t+1)(2t+3)}\right], \qquad \text{(A-3c)}
\end{aligned}
$$

$$I_{t,8}^{0n} = [\mathcal{N}_2]^{-1} \int_{-1}^{+1} (1-\eta^2)^{1/2} \frac{d\mathcal{S}_r^0(c,\eta)}{d\eta} P_{1+t}^1(\eta) d\eta$$
$$= d_{t+1}^{0n}, \tag{A-3d}$$

$$I_{t,9}^{0n} = [\mathcal{N}_2]^{-1} \int_{-1}^{+1} (1-\eta^2)^{3/2} \frac{d\mathcal{S}_r^0(c,\eta)}{d\eta} P_{1+t}^1(\eta) d\eta$$
$$= \frac{(t+3)(t+4)}{2t+5} \left[\frac{d_{t+1}^{0n}}{2t+3} - \frac{d_{t+3}^{0n}}{2t+7} \right]$$
$$- \frac{t(t-1)}{2t+1} \left[\frac{d_{t-1}^{0n}}{2t-1} - \frac{d_{t+1}^{0n}}{2t+3} \right], \tag{A-3e}$$

$$I_{t,10}^{0n} = [\mathcal{N}_2]^{-1} \int_{-1}^{+1} (1-\eta^2)^{5/2} \frac{d\mathcal{S}_r^0(c,\eta)}{d\eta} P_{1+t}^1(\eta) d\eta$$
$$= I_{t,9}^{0n} - \frac{(t+3)(t+4)(t+5)}{(2t+5)(2t+7)} \cdot \left[\frac{(t+1) d_{t+1}^{0n}}{(2t+3)(2t+5)} \right.$$
$$+ \frac{1}{2t+7} \left(\frac{t+6}{2t+9} - \frac{t+1}{2t+5} \right) d_{t+3}^{0n} - \left. \frac{(t+6) d_{t+5}^{0n}}{(2t+11)(2t+9)} \right]$$
$$- \frac{t(t+3)}{2t+3} \left(\frac{t+4}{2t+5} - \frac{t-1}{2t+1} \right) \cdot \left[\frac{(t-1) d_{t-1}^{0n}}{(2t-1)(2t+1)} \right.$$
$$+ \frac{1}{2t+3} \left(\frac{t+4}{2t+5} - \frac{t-1}{2t+1} \right) d_{t+1}^{0n} - \left. \frac{(t+4) d_{t+3}^{0n}}{(2t+7)(2t+5)} \right]$$
$$+ \frac{t(t-1)(t-2)}{(2t+1)(2t-1)} \cdot \left[\frac{(t-3) d_{t-3}^{0n}}{(2t-5)(2t-3)} \right.$$
$$+ \frac{1}{2t-1} \left(\frac{t+2}{2t+1} - \frac{t-3}{2t-3} \right) d_{t-1}^{0n} - \left. \frac{(t+2) d_{t+1}^{0n}}{(2t+3)(2t+1)} \right], \tag{A-3f}$$

and for even $(n-m)+t$:

$$I_{t,6}^{0n} = I_{t,7}^{0n} = I_{t,8}^{0n} = I_{t,9}^{0n} = I_{t,10}^{0n} = 0, \tag{A-4a}$$
$$I_{t,2}^{0n} = [\mathcal{N}_2]^{-1} \int_{-1}^{+1} (1-\eta^2)^{1/2} \mathcal{S}_r^0(c,\eta) P_{1+t}^1(\eta) d\eta$$
$$= \frac{d_t^{0n}}{(2t+1)} - \frac{d_{t+2}^{0n}}{(2t+5)}, \tag{A-4b}$$

$$I_{t,3}^{0n} = [\mathcal{N}_2]^{-1} \int_{-1}^{+1} (1-\eta^2)^{3/2} \mathcal{S}_r^0(c,\eta) P_{1+t}^1(\eta) d\eta$$
$$= \frac{(t+3)(t+4)}{(2t+5)} \left[\frac{d_t^{0n}}{(2t+1)(2t+3)} - \frac{2d_{t+2}^{0n}}{(2t+3)(2t+7)} + \frac{d_{t+4}^{0n}}{(2t+7)(2t+9)} \right] - \frac{t(t-1)}{(2t+1)} \cdot \left[\frac{d_{t-2}^{0n}}{(2t-3)(2t-1)} - \frac{2d_t^{0n}}{(2t-1)(2t+3)} + \frac{d_{t+2}^{0n}}{(2t+3)(2t+5)} \right], \tag{A-4c}$$

$$I_{t,4}^{0n} = [\mathcal{N}_2]^{-1} \int_{-1}^{+1} (1-\eta^2)^{5/2} \mathcal{S}_r^0(c,\eta) P_{1+t}^1(\eta) d\eta$$
$$= I_{t,3}^{0n} - \frac{(t+3)(t+4)(t+5)(t+6)}{(2t+5)(2t+7)(2t+9)} \cdot \left[\frac{d_{t+2}^{0n}}{(2t+5)(2t+7)} - \frac{2d_{t+4}^{0n}}{(2t+7)(2t+11)} + \frac{d_{t+6}^{0n}}{(2t+11)(2t+13)} \right]$$
$$- \frac{(t+3)(t+4)}{2t+5} \cdot \left[\frac{(t+1)(t+5)}{(2t+5)(2t+7)} + \frac{3t}{(2t+1)(2t+5)} \right] \cdot \left[\frac{d_t^{0n}}{(2t+1)(2t+3)} - \frac{2d_{t+2}^{0n}}{(2t+3)(2t+7)} + \frac{d_{t+4}^{0n}}{(2t+7)(2t+9)} \right]$$
$$- \frac{t(t-1)}{2t+1} \cdot \left[\frac{3(t+3)}{(2t+1)(2t+5)} - \frac{(t+2)(t-2)}{(2t+1)(2t-1)} \right] \cdot \left[\frac{d_{t-2}^{0n}}{(2t-3)(2t-1)} - \frac{2d_t^{0n}}{(2t+3)(2t-1)} + \frac{d_{t+2}^{0n}}{(2t+3)(2t+5)} \right]$$
$$+ \frac{(t(t-1)(t-2)(t-3)}{(2t+1)(2t-1)(2t-3)} \cdot \left[\frac{d_{t-4}^{0n}}{(2t-7)(2t-5)} - \frac{2d_{t-2}^{0n}}{(2t-1)(2t-5)} + \frac{d_t^{0n}}{(2t+1)(2t-1)} \right], \tag{A-4d}$$

$$I_{t,11}^{0n} = [\mathcal{N}_2]^{-1} \int_{-1}^{+1} \eta (1-\eta^2)^{1/2} \frac{d\mathcal{S}_r^0(c,\eta)}{d\eta} P_{1+t}^1(\eta) d\eta$$
$$= \frac{(t+3)}{(2t+5)} d_{t+2}^{0n} + \frac{t}{(2t+1)} d_t^{0n}, \tag{A-4e}$$

$$I_{t,12}^{0n} = \int_{-1}^{+1} \eta (1-\eta^2)^{3/2} \frac{d\mathcal{S}_r^0(c,\eta)}{d\eta} P_{1+t}^1(\eta) d\eta$$

$$= \frac{(t+3)(t+4)(t+5)}{(2t+5)(2t+7)}\left(\frac{d_{t+2}^{0n}}{(2t+5)} - \frac{d_{t+4}^{0n}}{(2t+9)}\right) + \frac{3t(t+3)}{(2t+1)(2t+5)}\left(\frac{d_{t}^{0n}}{(2t+1)} - \frac{d_{t+2}^{0n}}{(2t+5)}\right) - \frac{t(t-1)(t-2)}{(2t-1)(2t+1)}\left(\frac{d_{t-2}^{0n}}{(2t-3)} - \frac{d_{t}^{0n}}{(2t+1)}\right). \quad \text{(A-4f)}$$

The normalized coefficients $\mathcal{N}_1$ and $\mathcal{N}_2$ are given by

$$\mathcal{N}_1 = N_{m-1,m-1+t} = \frac{2}{2t+2m-1}\frac{(t+2m-2)!}{t!}, \quad \text{(A-5a)}$$

$$\mathcal{N}_2 = N_{1,1+t} = \frac{2}{2t+3}\frac{(t+2)!}{t!}. \quad \text{(A-5b)}$$

APPENDIX B: EXPRESSIONS OF $\mathcal{U}_{\substack{e\\o}}^{q(i),t}{}_{mn\theta}$, $\mathcal{U}_{\substack{e\\o}}^{q(i),t}{}_{mn\phi}$, $\mathcal{V}_{\substack{e\\o}}^{q(i),t}{}_{mn\theta}$, AND $\mathcal{V}_{\substack{e\\o}}^{q(i),t}{}_{mn\phi}$ ($q = z, \pm$, AND $i = 1, 2$)

$$\mathcal{U}_{\substack{e\\o}}^{z(i),t}{}_{mn\theta}(c) = \left(2mR_{mn}^{(i)}(c,\xi_0)\right) \cdot \left[(\xi_0^2-1)^2 I_{t,5}^{mn}(c) + 2(\xi_0^2-1)I_{t,6}^{mn}(c) + I_{t,7}^{mn}(c)\right], \quad \text{(B-1a)}$$

$$\mathcal{V}_{\substack{e\\o}}^{z(i),t}{}_{mn\theta}(c) = \frac{2}{c}\left\{\left[(\xi_0^2-1)^2\frac{dR_{mn}^{(i)}(c,\xi_0)}{d\xi_0}\right] I_{t,11}^{mn}(c) + \left[(\xi_0^2-1)\frac{dR_{mn}^{(i)}(c,\xi_0)}{d\xi_0} + 2\xi_0 R_{mn}^{(i)}(c,\xi_0)\right] I_{t,12}^{mn}(c) - (\xi_0^2-1)\cdot\left[\xi_0\left(\lambda_{mn} - c^2\xi_0^2 - \frac{m^2}{\xi_0^2-1}\right)R_{mn}^{(i)} - (\xi_0^2+1)\frac{dR_{mn}^{(i)}(c,\xi_0)}{d\xi_0}\right] I_{t,2}^{mn}(c) - \left[\xi_0\left(\lambda_{mn} - c^2\xi_0^2\right)R_{mn}^{(i)} + (\xi_0^2-1)\frac{dR_{mn}^{(i)}(c,\xi_0)}{d\xi_0}\right] I_{t,3}^{mn}(c) + \left[m^2\xi_0(\xi_0^2-1)R_{mn}^{(i)}(c,\xi_0)\right] I_{t,1}^{mn}(c)\right\}, \quad \text{(B-1b)}$$

$$\mathcal{U}_{\substack{e\\o}}^{z(i),t}{}_{mn\phi}(c) = R_{mn}^{(i)}(c,\xi_0) I_{t,12}^{mn}(c) - \xi_0\frac{dR_{mn}^{(i)}(c,\xi_0)}{d\xi_0} I_{t,3}^{mn}(c), \quad \text{(B-1c)}$$

$$\mathcal{V}^{z(i),t}_{\substack{e\\o}mn\phi}(c) = \frac{m}{c}\left\{\left[\frac{\xi_0}{\xi_0^2-1}R^{(i)}_{mn}(c,\xi_0)\right]I^{mn}_{t,9}(c) + \frac{dR^{(i)}_{mn}(c,\xi_0)}{d\xi_0}I^{mn}_{t,6}(c)\right\}, \tag{B-1d}$$

$$\begin{aligned}
\mathcal{U}^{\pm(i),t}_{\substack{e\\o}mn\theta}(c) &= \left(\frac{dR^{(i)}_{mn}(c,\xi_0)}{d\xi_0} \mp \frac{m\xi_0}{\xi_0^2-1}R^{(i)}_{mn}(c,\xi_0)\right)\\
&\quad\cdot\left[(\xi_0^2-1)^2 I^{mn}_{t,2}(c) + 2(\xi_0^2-1)I^{mn}_{t,3}(c) + I^{mn}_{t,4}(c)\right], \quad \text{(B-2a)}\\
\mathcal{V}^{\pm(i),t}_{\substack{e\\o}mn\theta}(c) &= \frac{1}{c}\left\{\left\{\left[(\xi_0^2-1)\left(\lambda_{mn} - c^2\xi_0^2 + \frac{m^2}{\xi_0^2-1}\right) - 2m(m\pm1)\right]\right.\right.\\
&\quad\cdot R^{(i)}_{mn}(c,\xi_0) - \xi_0(\xi_0^2-1)\frac{dR^{(i)}_{mn}(c,\xi_0)}{d\xi_0}\left.\right\}I^{mn}_{t,6}(c)\\
&\quad\mp\left[(m\pm1)(\xi_0^2-1)R^{(i)}_{mn}(c,\xi_0)\right]I^{mn}_{t,8}(c)\\
&\quad+\left[\left(\lambda_{mn} - c^2\xi_0^2 \mp \frac{m}{\xi_0^2-1}\right)R^{(i)}_{mn}(c,\xi_0)\right.\\
&\quad\left.+\,\xi_0\frac{dR^{(i)}_{mn}(c,\xi_0)}{d\xi_0}\right]I^{mn}_{t,7}(c) + \left[\xi_0(\xi_0^2-1)\frac{dR^{(i)}_{mn}(c,\xi_0)}{d\xi_0}\right.\\
&\quad\left.-\,(3\pm2m)R^{(i)}_{mn}(c,\xi_0)\right]I^{mn}_{t,9}(c) + \left[\xi_0\frac{dR^{(i)}_{mn}(c,\xi_0)}{d\xi_0}\right.\\
&\quad\left.+\left(2\mp\frac{m}{\xi_0^2-1}\right)R^{(i)}_{mn}(c,\xi_0)\right]I^{mn}_{t,10}(c)\\
&\quad-\left[m(m\pm1)(\xi_0^2-1)R^{(i)}_{mn}(c,\xi_0)\right]I^{mn}_{t,5}(c)\Big), \quad \text{(B-2b)}
\end{aligned}$$

$$\mathcal{U}^{\pm(i),t}_{\substack{e\\o}mn\phi}(c) = (\xi_0^2-1)\frac{dR^{(i)}_{mn}(c,\xi_0)}{d\xi_0}I^{mn}_{t,6}(c) + \xi_0 R^{(i)}_{mn}(c,\xi_0)I^{mn}_{t,9}(c), \tag{B-2c}$$

$$\begin{aligned}
\mathcal{V}^{\pm(i),t}_{\substack{e\\o}mn\phi}(c) &= \frac{1}{c}\left\{\left[m(m\pm1)R^{(i)}_{mn}(c,\xi_0)\right]I^{mn}_{t,1}(c)\right.\\
&\quad+\left[(1\pm m)R^{(i)}_{mn}(c,\xi_0)\right]I^{mn}_{t,11}(c) - \left[c^2R^{(i)}_{mn}(c,\xi_0)\right]I^{mn}_{t,3}(c)\\
&\quad+\left[\left(-c^2(\xi_0^2-1) + \frac{m(m\pm1)}{\xi_0^2-1}\right)R^{(i)}_{mn}(c,\xi_0)\right]I^{mn}_{t,2}(c)\\
&\quad\left.-\left[(1\pm m)\xi_0\frac{dR^{(i)}_{mn}(c,\xi_0)}{d\xi_0}\right]I^{mn}_{t,2}(c)\right\}. \quad \text{(B-2d)}
\end{aligned}$$

REFERENCES

1. Jensen, M. A., and Y. Rahmat-Samii, "EM interaction of handset antennas and a human in personal communications," *Proc. IEEE,* Vol. 83, 7–17, 1995.
2. Okoniewski, M., and M. A. Stuchly, "A study of the handset antenna and human body interaction," *IEEE Trans. Microwave Theory Tech.,* Vol. MTT-44, 1855–1864, 1996.
3. Li, L. W., P. S. Kooi, M. S. Leong, H. M. Chan, and T. S. Yeo, "FD-TD analysis of electromagnetic interactions between handset antennas and the human head," in *The 1997 Asia-Pacific Microwave Conference,* (APMC'97), Vol. 3rd of 3, 1189–1192, Hong Kong, December 2–5, 1997.
4. Scott, J. A., "A finite element model of heat transport in the human eye," *Physics in Medicine and Biology,* Vol. 33, 227–241, 1988.
5. Dimbylow, P. J., and O. P. Grandhi, "Finite-difference time-domain calculations of SAR in a realistic heterogeneous model of the head foe plane-wave exposure from 600 MHz to 3 GHz," *Physics in Medicine and Biology,* Vol. 36, 1075–1089, 1991.
6. Chen, H. Y., and H. H. Wang, "Current and SAR induced in a human head model by the electromagnetic fields irradiated from a cellular phone," *IEEE Trans. Microwave Theory Tech.,* Vol. MTT-42, 2249–2254, 1994.
7. Dimbylow, P. J., and S. M. Mann, "SAR calculations in an anatomically realistic model of the head for mobile communication transceivers at 900 MHz and 1.8 GHz," *Physics in Medicine and Biology,* Vol. 39, 1537–1553, 1994.
8. Watanabe, S., M. Taki, and O. Fujiwara, "Characteristics of the SAR distributions in a head exposed to electromagnetic fields radiated by a hand-held portable radio," *IEEE Trans. Microwave Theory Tech.,* Vol. MTT-44, 1874–1883, 1996.
9. Gandhi, O. P., G. Lazzi, and C. M. Furse, "Electromagnetic absorption in the human head and neck for mobile telephones at 835 and 1900 MHz," *IEEE Trans. Microwave Theory Tech.,* Vol. MTT-44, 1884–1896, 1996.
10. Livesay, D. E., and K. M. Chen, "Electromagnetic fields induced inside arbitrarily shaped biological bodies," *IEEE Trans. Microwave Theory Tech.,* Vol. MTT-22, 1273–1280, 1974.
11. Stuchly, M. A., R. J. Spiegel, S. S. Stuchly, and A. Kraszewski, "Exposure of man in the near-field of a resonant dipole: comparison between theory and measurements," *IEEE Trans. Microwave Theory Tech.,* Vol. MTT-34, 26–31, 1986.

12. Weil, C. M., "Absorption characteristics of multilayered sphere models exposed to UHF/microwave radiation," *IEEE Trans. Biomed. Eng.,* Vol. BME-22, 468–476, 1975.
13. Kritikos, H. N., and H. P. Schwan, "The distribution of heating potential inside lossy spheres," *IEEE Trans. Biomed. Eng.,* Vol. BME-22, 457–463, 1975.
14. Hizal, A., and Y. K. Baykal, "Heat potential distribution in an inhomogeneous spherical model of a cranial structure exposed to microwaves due to loop or dipole antennas," *IEEE Trans. Microwave Theory Tech.,* Vol. MTT-26, 607–612, 1978.
15. Kamimura, Y., H. Tohyama, and K. Matsumura, "Energy deposition in a multilayered spherical model of a human head exposed to a shorten dipole," in *Proc. of 1995 Asia-Pacific Microwave Conference,* (APMC'95), KAIST, Vol. 1st of 2, 260–263, Taejon, Korea, October 10–13, 1995,
16. Dalmas, J., and R. Deleuil, "Multiple scattering of electromagnetic waves from two infinitely conducting prolate spheroids which are centered in a plane perpendicular to their axes of revolution," *Radio Sci.,* Vol. 20, 575–581, 1985.
17. Sinha, B. P., and R. H. MacPhie, "Electromagnetic plane wave scattering by a system of two parallel conducting spheroids," *IEEE Trans. Antennas Propagat.,* Vol. AP-31, 294–304, 1983.
18. Cooray, M. F. R., and I. R. Ciric, "Scattering of electromagnetic waves by a system of two dielectric spheroids of arbitrary orientation," *IEEE Trans. Antennas Propagat.,* Vol. AP-39, 680–684, 1991.
19. Cooray, M. F. R., and I. R. Ciric, "Scattering of electromagnetic waves by a coated dielectric spheroid," *J. Electromagn. Waves Applic.,* Vol. 6, 1491–1507, 1992.
20. Flammer, C., *Spheroidal Wave Functions,* California: Stanford Univ. Press, 1957.
21. Do-Nhat, T., and R. H. MacPhie, "Accurate values of prolate spheroidal radial functions of the second kind," *Can. J. Phys.,* Vol. 75, 671–675, 1997.
22. Sinha, B. P., and R. H. MacPhie, "Electromagnetic scattering by prolate spheroids for plane waves with arbitrary polarization and angle of incidence," *Radio Sci.,* Vol. 12, 171–184, 1977.
23. Stratton, J. A., P. M. Morse, L. J. Chu, J. D. C. Little, and F. J. Corbato, *Spheroidal wave functions,* New York: John Wiley & Sons, 1956.

24. Johnson, C. C., C. H. Durney, and H. Massoudi, "Long-wavelength electromagnetic power absorption in prolate spheroidal models of man and animals," *IEEE Trans. Microwave Theory Tech.,* Vol. MTT-23, 739–747, 1975.
25. Iskander, M. F., P. W. Barber, C. H. Durney, and H. Massoudi, "Irradiation of prolate spheroidal models of humans in the near field of a short electric dipole," *IEEE Trans. Microwave Theory Tech.,* Vol. MTT-28, 801–807, 1980.
26. Lakhtakia, A., M. F. Iskander, C. H. Durney, and H. Massoudi, "Near-field absorption in prolate spheroidal models of humans exposed to a small loop antenna of arbitrary orientation," *IEEE Trans. Microwave Theory Tech.,* Vol. MTT-29, 588–594, 1981.
27. Lakhtakia, A., M. F. Iskander, C. H. Durney, and H. Massoudi, "Irradiation of prolate spheroidal models of humans and animals in the near field of a small loop antenna," *Radio Sci.,* Vol. 17, 77s–84s, 1982.
28. Uzunoglu, N. K., and E. A. Angelikas, "Field distributions in a three-layer prolate spheroidal human body model for a loop antenna irradiation," *IEEE Trans. Antenna and Propagat.,* Vol. AP-35, 1180–1185, 1987.
29. Schwan, H. P., "Electrical properties of tissues and cells," *Advan. Bio. Med. Phys.,* Vol. 5, 147–209, 1957.
30. Schman, H. P., "Interaction of microwave and radio frequency radiation with biological systems," *IEEE Trans. Microwave Theory Tech.,* vol. MTT-19, 146–152, 1971.
31. Gabriel, C., "Dielectric properties of biological material," in *The NATO Conference,* Rome, Italy, May 18, 1993.
32. Stratton, J. A., *Electromagnetic Theory,* New York: McGraw-Hill, 1941.
33. Tai, C. T., *Dyadic Green's Functions in Electromagnetic Theory,* Piscataway, New Jersey: IEEE Press, The 2nd edition, 1994.
34. Kong, J. A., *Electromagnetic Wave Theory,* John Wiley & Sons, Inc., The 2nd edition, 1986.
35. Li, L. W., M. S. Leong, P. S. Kooi, T. S. Yeo, and X. Ma, "On the spheroidal vector wave eigenfunction expansion of dyadic Green's functions for a spheroid," in *Proc. of 1995 Asia-Pacific Microwave Conference,* (APMC'95), KAIST, Vol. 2nd of 2, 524–527, Taejon, Korea, October 10–13, 1995.

36. Asano, S., and G. Yamamoto, "Light scattering by a spheroidal particle," *Appl. Opt.,* Vol. 14, 29–49, 1975.
37. Li, L. W., M. S. Leong, P. S. Kooi, and T. S. Yeo, "Spheroidal vector wave eigenfunction expansion of dyadic Green's functions for a dielectric spheroid," accepted by *IEEE Trans. Antennas Propagt.,* July 1998.
38. Oguchi, T., "Eigenvalues of spheroidal wave functions and their branch points for complex values of propagation constants," *Radio Sci.,* Vol. 5, 1207–1214, 1970.
39. Jen, L., and C. S. Hu, "Spheroidal wave functions of large frequency parameters $c = kf$ and the radiation fields of a metallic prolate spheroid excited by any circumferential slot," *IEEE Trans. Antennas Propagat.,* Vol. AP-31, 382–389, 1983.
40. Li, L. W., T. S. Yeo, P. S. Kooi, M. S. Leong, and K. Y. Tan, "Exact computations of spheroidal harmonics with complex argument: A comparative study with an algorithm," *Physical Review E,* Vol. 58, No. 5, November 1998.